
Journal of Coordination Chemistry
Publication details, including instructions for authors and subscription information:
http://www.tandfonline.com/loi/gcoo20

# Synthesis, characterization, molecular modeling, and thermal analyses of bioactive Co(II) and Cu(II) complexes with diacetylmonoxime and different amines

Abdalla M. Khedr [a], M. Gaber [a] & Hatem A. Diab [a]
[a] Chemistry Department, Faculty of Science, Tanta University, Tanta, Egypt
Published online: 05 Apr 2012.

To cite this article: Abdalla M. Khedr, M. Gaber & Hatem A. Diab (2012) Synthesis, characterization, molecular modeling, and thermal analyses of bioactive Co(II) and Cu(II) complexes with diacetylmonoxime and different amines, Journal of Coordination Chemistry, 65:10, 1672-1684, DOI: 10.1080/00958972.2012.678338

To link to this article: http://dx.doi.org/10.1080/00958972.2012.678338

*Journal of Coordination Chemistry*
Vol. 65, No. 10, 20 May 2012, 1672–1684



# Synthesis, characterization, molecular modeling, and thermal analyses of bioactive Co(II) and Cu(II) complexes with diacetylmonoxime and different amines

ABDALLA M. KHEDR*, M. GABER and HATEM A. DIAB

Chemistry Department, Faculty of Science, Tanta University, Tanta, Egypt

(*Received 24 October 2011; in final form 28 February 2012*)

Condensation of diacetylmonoxime with 2-amino-5-mercapto-1,3,4-thiadiazole, 2-amino-1,3,4-thiadiazole or 3-amino-5-methylisoxazole in the presence of Co(II) and Cu(II) salts with different anions produced nine complexes. The synthesized complexes have been characterized by elemental analyses, molar conductivities, thermal analyses, magnetic moments, IR, electron spin resonance, and UV-Vis spectral studies. The spectral data show that sulfur, oxygen, and nitrogen participate in chelation with the metal ions. The complexes are tetrahedral, octahedral, or square planar based on the amine used and the nature of anion. Molar conductance measurements of the complexes in DMF indicate non-electrolytes. CS Chem 3-D Ultra Molecular Modeling and Analysis Program has been used for optimization of the molecular structures of some complexes. *In vitro* cytotoxicities of the complexes were tested against different carcinoma cell lines. Antimicrobial activities of the complexes were screened against Gram-positive (*Staphylococcus aureus*), Gram negative bacteria (*Escherichia coli*), and fungal species (*Aspergillus flavus*, *Candida albicans*, and *Microsporum canis*).

*Keywords*: Synthesis; Characterization; Co(II) and Cu(II) complexes; Diacetylmonoxime



## 1. Introduction

Interest in 3-D metal complexes with biologically active heterocyclic ligands, in particular, with thiadiazoles and isoxazole, arises from potential applications in medicine and agriculture [1–6]. Chelating ligands containing O, S, and N donors show broad biological activity and are of special interest because of the variety of ways in which they are bonded to metal ions [7–9]. Oximes and their complexes have played a role in the development of transition metal chemistry [10–12]; oxime derivatives are very important in medicinal and chemical industries [13] with broad pharmacological activity, encompassing antibacterial, antidepressant, anti-carcinogenic, and antifungal activities [14–16]. Oximes are well known for their coordinating abilities and versatile behavior [17], but much remains to be learned about the types of structures that are

*Corresponding author. Email: abkhedr2001@yahoo.com


ISSN 0095-8972 print/ISSN 1029-0389 online 
http://dx.doi.org/10.1080/00958972.2012.678338

formed as well as the factors that dictate structure. In general, the oxime function coordinates to the metal ions in four ways (**I–IV**):

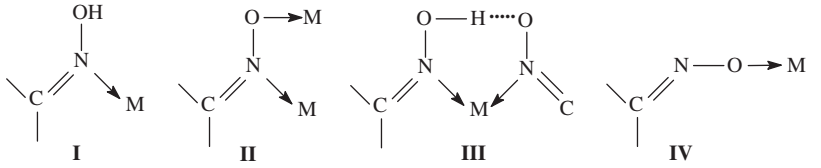


Coordination modes **I** and **III** are quite common among metal complexes but oxime is a poor donor unless it is part of a chelate ring [18].

We report here the synthesis, characterization, and biological activities of Co(II) and Cu(II) complexes with diacetylmonoxime (DAM) and 2-amino-5-mercapto-1,3,4-thiadiazole (2A5MT), 2-amino-1,3,4-thiadiazole (2AT) or 3-amino-5-methylisoxazole (3A5MO).



## 2. Experimental

All chemicals and solvents used were of reagent grade from Merck, Aldrich, or Sigma.

### 2.1. *Synthesis of metal complexes*

$(CH_3CO_2)_2Co \cdot 4H_2O$ (1.99 g, 10 mmol), $(CH_3CO_2)_2Cu \cdot H_2O$ (10 mmol, 2.00 g), $CuCl_2 \cdot H_2O$ (10 mmol, 1.52 g), or $Cu(NO_3)_2 \cdot 2H_2O$ (10 mmol, 1.46 g) were dissolved in 30 mL methanol and mixed with methanolic solution of diacetylmonoxime (10 mmol, 1.01 g). To this, a solution of 2-amino-5-mercapto-1,3,4-thiadiazole (10 mmol, 1.33 g), 2-amino-1,3,4-thiadiazole (10 mmol, 1.01 g), or 3-amino-5-methylisoxazole (10 mmol, 0.98 g) was added dropwise with constant stirring. The reaction mixtures were refluxed with stirring for 48 h. On cooling and concentration, colored solid metal complexes were precipitated, filtered off, washed with cold methanol, and dried under vacuum over dried silica gel. Purities of the complexes were checked by TLC and melting point constancy.

### 2.2. *Apparatus and working procedures*

Carbon, hydrogen, and nitrogen analyses were carried out at the Micro-analytical Unit of Tanta University and Cairo University. The molar conductivities of the complexes ($\Lambda_M$) were measured in DMF at room temperature using a conductance bridge of the type 523 conductometer. IR spectra were recorded in the 4000–200 $cm^{-1}$ region with a Perkin-Elmer 1430 double beam spectrophotometer as KBr discs. UV-Vis spectra were measured from 900 to 190 nm by a Shimadzu UV-Vis 160A double beam spectrophotometer using Nujol mulls. Magnetic susceptibility measurements at room temperature were performed by modified Gouy's technique using magnetic susceptibility balance (Johnson Matthey) 436 Devon Park Drive, Wayne, PA 19087, USA (60 Hz).

Electron spin resonance (ESR) spectra were recorded on a Jeol spectrometer model JES-FE2XG equipped with an E101 microwave bridge. Measurements were done in the X-band on microcrystalline powder at room temperature using DPPH as standard. Thermogravimetric analysis (TGA) and differential thermal analysis (DTA) measurements were recorded on Shimadzu TG-50 and DT-50 thermal analyzers.

### 2.3. *Molecular modeling*

The molecular structures of the complexes were supported by molecular modeling of some representative complexes using CS Chem 3-D Ultra Molecular Modeling and Analysis Program [19], an interactive graphics program that allows rapid structure building, geometry optimization with minimum energy, and molecular display. It has ability to handle transition metal complexes [20–23]. The correct stereochemistry was assured through manipulation and modification of the molecular coordinates to obtain reasonable, low energy molecular geometries. The potential energy of the molecule was the sum of the following terms:

$$E = E_{str} + E_{ang} + E_{tor} + E_{vdw} + E_{oop} + E_{ele},$$

where all $E$'s represent the energy values corresponding to the given types of interaction (kcal $mol^{-1}$). The subscripts str, ang, tor, vdw, oop, and ele denote bond stretching, angle bending, torsion, van der Waals interactions, out-of-plane bending, and electronic interaction, respectively. The molecular mechanics describe the application of classical mechanics for the determination of molecular equilibrium structures, enabling calculation of the total static energy of a molecule in terms of deviations from reference unstrained bond lengths, angles, and torsions plus non-bonded interactions. It has been found that off-diagonal terms are usually largest when neighboring atoms are involved, and so we have to take account of non-bonded interactions, but only between nearest neighbors [23].

### 2.4. *Measurement of the potential cytotoxicity*

*In vitro* potential cytotoxicity of the complexes was tested using the method of Skehan *et al.* [24] in Pharmacology Unit, Cancer Biology Department, National Cancer Institute, Cairo University. Different concentrations of the compounds (0, l, 2.5, 5, l0, 15, 20, and 50 $\mu g\,mL^{-1}$) were added to the cell monolayer and triplicate wells were prepared for each individual dose. Monolayer cells were incubated with the compounds for 48 h at 37°C in atmosphere of 5% $CO_2$. After 48 h, cells were fixed, washed, and stained with Sulfo-Rhodamine-B (SRB) stain. Color intensity was measured in a microplate reader. The relation between fraction of live cells and drug concentrations is plotted to get the survival curve of each tumor cell line after treatment with the specified compound.

### 2.5. In vitro *antibacterial and antifungal assay*

Antimicrobial activities of the tested samples were determined using a modified Kirby–Bauer disc diffusion method [25] in the Micro-analytical Unit of Cairo University.

100 μL of the test bacteria/fungi were grown in 10 mL of fresh media until they reached a count of approximately 108 cells $mL^{-1}$ for bacteria or 105 cells $mL^{-1}$ for fungi [26]. 100 μL of microbial suspension was spread onto agar plates corresponding to the broth in which they were maintained. Isolated colonies of each organism were selected from primary agar plates and tested for susceptibility by the disc diffusion method [27–29]. Plates were inoculated with filamentous fungi such as *Aspergillus flavus* at 25°C for 48 h; Gram (+) bacteria such as *Staphylococcus aureus* and Gram (−) bacteria such as *Escherichia coli* were incubated at 35–37°C for 24–48 h and yeast such as *Candida albicans* and *Microsporum canis* incubated at 30°C for 24–48 h, and then the diameters of the inhibition zones were measured in millimeters [30]. When an organism is placed on the agar it will not grow in the area around the disc if it is susceptible to the chemical. This area of no growth around the disc is known as a "zone of inhibition" or "clear zone." For disc diffusion, the zone diameters were measured with slipping calipers of the National Committee for Clinical Laboratory Standards [30]. Agar-based methods such as Etest and disc diffusion can be good alternatives because they are simpler and faster than broth-based methods [31, 32].



## 3. Results and discussion

The isolated complexes are stable in air and soluble in polar organic solvents. Molecular formulae, colors, formula weights obtained from thermal analysis, elemental analyses, and molar conductances of metal chelates are listed in table 1. Metal contents were estimated complexometrically using standard EDTA titration [33]. The calculated and found values of C, H, N, and metal are in satisfactory agreement supporting the suggested molecular formulae. The molar conductances of the complexes in DMF (table 1) indicate that they are non-electrolytes having $\Delta_M$ in the range 4.0–9.1 $Ohm^{-1}\,cm^2\,mol^{-1}$ [34].

### 3.1. *IR spectra*

Tentative assignment of the most characteristic IR bands of **$T_1$**–**$T_9$**, diacetylmonoxime, 2-amino-5-mercapto-1,3,4-thiadiazole, 2-amino-1,3,4-thiadiazole, and 3-amino-5-methylisoxazole are given in table 2. The strong absorption at 1676 $cm^{-1}$ in the spectrum of diacetylmonoxime due to $\nu$(C=O) disappeared in spectra of all complexes, indicating the absence of residual C=O. The $\nu(NH_2)$ bands observed in the amine spectra at 3210–3339 $cm^{-1}$ shifted to higher values in spectra of **$T_2$**–**$T_5$** and did not appear in spectra of **$T_1$** and **$T_6$**–**$T_9$**. The $\nu$(S–H) at 2642 $cm^{-1}$ for 2-amino-5-mercapto-1,3,4-thiadiazole disappeared in spectra of **$T_1$** and **$T_2$** and appeared at 2557 and 2561 $cm^{-1}$ in spectra of **$T_3$** and **$T_4$**. All the complexes show a strong absorption at 1567–1629 $cm^{-1}$ attributed to coordinated C=N, indicating condensation of the carbonyl and amino groups [35].

For **$T_1$**, **$T_2$**, and **$T_6$**–**$T_8$**, acetates display asymmetric and symmetric vibrations at 1569–1629 (s) $cm^{-1}$ and 1364–1414 $cm^{-1}$, respectively, with $\Delta\nu = 205$–$215\,cm^{-1}$ characteristic of monodentate coordination [36, 37]. The band at 1364–1414 $cm^{-1}$ is due to $\nu_S(CO_2)$ of acetate. Chloro complexes **$T_3$**, **$T_5$**, and **$T_9$** showed bands at 220, 292, and

Table 1. Physical characteristics, analytical, and molar conductance data of $\mathbf{T_1}$–$\mathbf{T_9}$.

| No. | Molecular formula (empirical formula) | Color ($\Delta_m$ = molar conductance; $\Omega^{-1}\,cm^2\,mol^{-1}$) | Mol. weight (melting point °C) | Elemental analysis | | | |
|---|---|---|---|---|---|---|---|
| | | | | C (%) Calcd (Found) | H (%) Calcd (Found) | N (%) Calcd (Found) | Metal content Calcd (Found) |
| $\mathbf{T_1}$ | $[(DAM)_2(2A5MT)_2Co_3(AcO)_2(H_2O)_2]\cdot 4H_2O$ ($C_{16}H_{30}Co_3N_8S_4O_{12}$) | Reddish-brown (9.1) | 831.49 (300) | 23.16 (23.65) | 3.64 (4.07) | 13.52 (14.04) | 21.29 (21.27) |
| $\mathbf{T_2}$ | $[(DAM)(2A5MT)_3Cu_3(AcO)_2]\cdot 7H_2O$ ($C_{14}H_{30}Cu_3N_{10}S_6O_{12}$) | Green (8.2) | 913.45 (268) | 18.40 (18.26) | 3.28 (3.25) | 15.34 (15.04) | 20.88 (20.72) |
| $\mathbf{T_3}$ | $[(DAM)(2^a5MT)_4Cu_2Cl_2(H_2O)_4]\cdot 5H_2O$ ($C_{12}H_{33}Cu_2N_{13}S_8O_{10}Cl_2$) | Yellow (8.0) | 973.95 (190) | 14.79 (14.85) | 3.39 (2.89) | 18.70 (18.51) | 13.06 (13.18) |
| $\mathbf{T_4}$ | $[(DAM)(2A5MT)_4Cu_3(NO_3)_2]$ ($C_{12}H_{13}Cu_3N_{15}S_8O_7$) | Yellow (5.2) | 926.45 (171) | 15.54 (15.15) | 1.40 (1.74) | 22.66 (22.55) | 20.58 (20.41) |
| $\mathbf{T_5}$ | $[(DAM)(2AT)_4Cu_4Cl_8(H_2O)]\cdot 2H_2O$ ($C_{12}H_{21}Cu_4N_{13}S_4O_3Cl_8$) | Green (6.1) | 1061.43 (220) | 13.56 (13.36) | 1.97 (2.15) | 17.14 (17.14) | 23.93 (23.87) |
| $\mathbf{T_6}$ | $[(DAM)_2(2A5MO)Cu_2(AcO)_2]\cdot 4H_2O$ ($C_{16}H_{30}Cu_2N_4O_{12}$) | Brown (4.0) | 597.53 (300) | 32.15 (32.43) | 5.02 (5.08) | 9.37 (9.58) | 21.28 (21.43) |
| $\mathbf{T_7}$ | $[(DAM)_2(2AT)Co_2(AcO)_2]\cdot 7H_2O$ ($C_{14}H_{33}Co_2N_5SO_{14}$) | Reddish-brown (8.0) | 645.36 (300) | 26.05 (26.18) | 5.11 (5.45) | 10.85 (10.75) | 18.27 (18.08) |
| $\mathbf{T_8}$ | $[(DAM)(2AT)Cu(AcO)(H_2O)]\cdot H_2O$ ($C_8H_{14}CuN_4SO_5$) | Green (6.0) | 341.83 (300) | 28.10 (27.93) | 4.09 (3.64) | 16.39 (16.82) | 18.60 (18.78) |
| $\mathbf{T_9}$ | $[(DAM)(2A5MO)CuCl_2]\cdot 4H_2O\cdot 2CH_3OH$ ($C_{10}H_{27}CuN_3O_8Cl_2$) | Brown (9.0) | 451.79 (142) | 26.58 (26.61) | 5.98 (5.61) | 9.30 (9.05) | 14.7 (14.51) |

The yield for the synthesized complexes was 78%–84%. All the synthesized complexes decompose without melting. DAM = diacetylmonoxime; 2A5MT = 2-amino-5-mercapto-1,3,4-thiadiazole; 2AT = 2-amino-1,3,4-thiadiazole; 3A5MO = 3-amino-5-methylisoxazole.

Table 2. IR and UV-Vis spectral data as well as magnetic moment values of the complexes.

| No. | IR spectra ($\bar{\nu}$; $cm^{-1}$) | | | | | | | | Electronic spectra ($\bar{\nu}$; $cm^{-1}$) in Nujol mull | $\mu_{eff}$ (magnetic moment; B.M.) |
|---|---|---|---|---|---|---|---|---|---|---|
| | $\nu(OH/H_2O)$ | $\nu(NH_2)$ | $\nu$(C=N) Schiff | $\nu$(C=N) Ring | $\nu$(N–O) | $\nu$(C–S) | $\nu$(M–O) | $\nu$(M–N) | | |
| DAM | – | – | – | – | 937 | – | – | – | – | – |
| 3A5MT | – | 3339 | – | 1550 | – | 641 | – | – | – | – |
| 2AT | – | 3286 | – | 1509 | – | 682 | – | – | – | – |
| 3A5MO | – | 3210 | – | 1516 | – | – | – | – | – | – |
| **$T_1$** | 3369 | – | 1614 | 1522 | 1212 | 668 | 582 | 410 | 18,116; 20,410 | 4.73 |
| **$T_2$** | 3450 | 3279 | 1605 | 1510 | 1119 | 698 | 582 | 441 | 21,740 | 1.57 |
| **$T_3$** | 3410 | 3259 | 1602 | 1492 | 1181 | 694 | 581 | 428 | 15,150; 17,850; 21,270 | 1.66 |
| **$T_4$** | – | 3392 | 1600 | 1487 | 1140 | 689 | 583 | 435 | 20,830 | 1.72 |
| **$T_5$** | 3396 | 3240 | 1605 | 1522 | 1110 | 716 | 561 | 442 | 22,220 | 1.98 |
| **$T_6$** | 3409 | – | 1629 | 1554 | 1124 | – | 582 | 420 | 21,275 | 1.58 |
| **$T_7$** | 3424 | – | 1567 | 1414 | 1135 | 710 | 582 | 390 | 18,018; 20,000 | 4.77 |
| **$T_8$** | 3412 | – | 1613 | 1562 | 1132 | 693 | 583 | 408 | 18,180; 22,220 | 1.77 |
| **$T_9$** | 3437 | – | 1628 | 1545 | 1121 | – | 580 | 466 | 21,980 | 1.92 |

DAM = diacetylmonoxime; 2A5MT = 2-amino-5-mercapto-1,3,4-thiadiazole; 2AT = 2-amino-1,3,4-thiadiazole; 3A5MO = 3-amino-5-methylisoxazole.

222 $cm^{-1}$, respectively, assigned to M–Cl [38]. The spectrum of **$T_4$** showed bands at 1450 ($\nu_1$), 1362 ($\nu_2$), 1030 ($\nu_3$), and 710 $cm^{-1}$ ($\nu_4$) with $\nu_1$–$\nu_4$ separation of 740 $cm^{-1}$ characteristic of monodentate nitrate [37]. The absorption at 1212–1140 $cm^{-1}$ is assigned to $\nu$(N–O) [39]. The shift of these bands to high frequency is an indication of coordination of nitrogen of neutral oxime or coordination of the oxime [40]. These observations are confirmed by the appearance of non-ligand bands at 561–583 and 390–466 due to $\nu$(M–O) and $\nu$(M–N), respectively [41]. $\nu$(C–S) at 641 and 682 $cm^{-1}$ in spectra of 2-amino-5-mercapto-1,3,4-thiadiazole and 2-amino-1,3,4-thiadiazole shift to high frequencies, indicating participation of sulfur in coordination [42]. Except for **$T_4$**, all complexes display broad bands at 3369–3450 $cm^{-1}$ due to $\nu$(OH) from water [43]. This band is absent in the ligands and has been confirmed with TGA/DTA.



### 3.2. *ESR spectra*

X-band ESR spectra of powdered Cu(II) complexes **$T_2$**, **$T_3$**, and **$T_8$** have been recorded at room temperature (figure 1). ESR spectrum of **$T_2$** shows a sharp signal with $g_{eff}$, $g_{||}$, and $g_{\perp}$ values equal to 2.0880, 2.2680, and 2.0830. That $g_{||} > g_{\perp} > g_e$ (2.00023) shows the unpaired d-electron is in the $d_{x^2-y^2}$ orbital for complex having tetrahedral structure [44]. The spectrum of **$T_3$** displayed a sharp signal with $g_{eff}$, $g_{||}$, and $g_{\perp}$ values equal to 2.2356, 2.0835, and 2.2536. The ESR pattern and the fact that ESR parameters $g_{\perp} > g_{||} > 2.0023$ prove octahedral geometry and indicate that the unpaired d-electron is present in the $d_{z^2}$ orbital with slight distortion of the symmetry around the $z$-axis [45].

The $G$ factor defined as $G = (g_{||} - 2)/(g_{\perp} - 2)$ equals 3.2 and 3.3 for **$T_2$** and **$T_3$**, respectively. These values are less than 4.00, indicating the existence of an interaction between Cu(II) centers in the solid state [44].

ESR spectrum of Cu(II) complex **$T_8$** showed a broad signal with no hyperfine structure with $g_{eff}$ value 2.0719, which indicates that **$T_8$** has square-planar geometry [46].

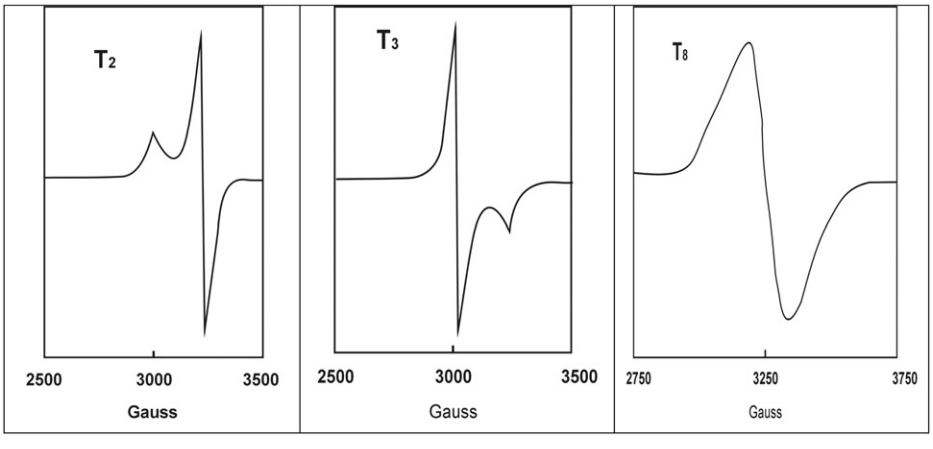


Figure 1. ESR spectra of solid Cu(II) complexes **$T_2$**, **$T_3$**, and **$T_8$** at 298 K.

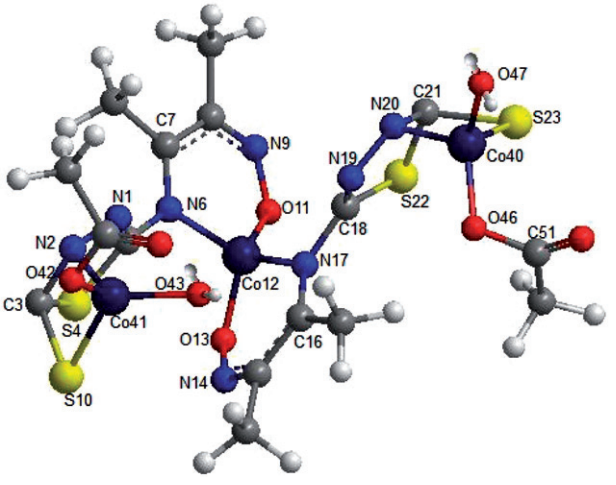


Figure 2. 3-D molecular modeling of $\mathbf{T_1}$.

### 3.3. *Molecular modeling and analysis of bonding modes*

Molecular mechanics attempts to reproduce molecular geometries, energies, and other features by adjusting bond length, bond angles, and torsion angles to equilibrium values that are dependent on the hybridization of an atom and its bonding scheme. To obtain structural details of these complexes, we have optimized the molecular structure of $\mathbf{T_1}$ (figure 2) and $\mathbf{T_6}$–$\mathbf{T_9}$ (Supplementary material) using CS Chem 3-D Ultra Molecular Modeling and Analysis Program [17]. For convenience, the atoms are numbered in Arabic numerals. Energy minimization was repeated several times to find the global minimum [47]. The energy minimization values for tetrahedral $\mathbf{T_1}$, $\mathbf{T_6}$, $\mathbf{T_7}$, and $\mathbf{T_9}$ are 165.454, 51.963, 53.391, and 18.455 kcal mol$^{-1}$ whereas the minimum energy value for square planar $\mathbf{T_8}$ is 24.091 kcal mol$^{-1}$. The energy minimization value of the complexes increases with increasing number of metal ions and is also affected by the nature of the metal. Bond lengths are in the range 1.786–2.202 Å. Molecular modeling for $\mathbf{T_1}$, $\mathbf{T_6}$, $\mathbf{T_7}$, and $\mathbf{T_9}$ shows the angles around metal ions are 91.53–115.7, indicating distorted tetrahedral geometry [21, 22, 47]. The bond angles around Cu(II) in $\mathbf{T_8}$ are 104.88°, 109.65°, 111.16°, and 109.70°, confirming square-planar geometry [17, 18]. The details of bond lengths and angles as per the 3-D molecular structures of the investigated complexes are given in "Supplementary material."

Based on the information gained from the above studies, the structure of the complexes under investigation can be represented (figure 2 and Supplementary material).

### 3.4. *Electronic spectra and magnetic data*

The electronic spectrum of Co(II) complex $\mathbf{T_1}$ displayed bands at 18116 and 20410 cm$^{-1}$ and $\mathbf{T_7}$ showed bands at 18,018 and 20,000 cm$^{-1}$, corresponding to $^4A_2 \rightarrow {}^4T_1(P)$ and $^4T_{1g}(F) \rightarrow {}^4T_{2g}$ transitions, respectively [48]. The shape of the spectra and magnetic moment values of $\mathbf{T_1}$ and $\mathbf{T_7}$ (4.73 and 4.77 B.M.) are consistent with tetrahedral

geometry around Co(II) [49] (table 2). $\mathbf{T_3}$ showed three bands at 21,270, 17,850, and 15,150 $cm^{-1}$ corresponding to the charge transfer, $^2B_{1g} \rightarrow {}^2E_g$ and $^2B_{1g} \rightarrow {}^2B_{2g}$ transitions [50]. The broadness of the band is due to the ligand field and the Jahn–Teller effect [51]. These observations and the magnetic moment value (1.76 B.M.) favor octahedral Cu(II) [50, 51]. $\mathbf{T_8}$ showed two bands at 18,180 and 22,220 $cm^{-1}$, assignable to $^2B_{1g} \rightarrow {}^2A_1$ and $^2B_{1g} \rightarrow {}^2E_g$ transitions in square-planar geometry [52]. The magnetic moment value of $\mathbf{T_8}$ equals 1.77 B.M. The spectra of the other Cu(II) complexes display a band at 20,830–22,220 $cm^{-1}$ due to $^2B_{2g} \rightarrow {}^2T_{2g}$ electronic transition in tetrahedral arrangement [49]. The room temperature magnetic moments of Cu(II) complexes (table 2) are 1.57–1.78 B.M. The magnetic moment values for Co(II) and Cu(II) complexes are lower than those for the spin only value of $d^7$ and $d^9$ ions, which indicates the existence of anti-ferromagnetic interactions between the metal ions in multinuclear complexes [53].



### 3.5. *Thermal analyses*

By thermal analyses of the metal complexes, information on their properties, nature of intermediate, and final products of their thermal decomposition can be obtained [54]. TGA and DTA curves were performed from ambient temperature to 1000°C under $N_2$ gas at a heating rate of 10°C $min^{-1}$. From TGA curves, the mass loss was calculated for the different steps and compared with those theoretically calculated for the suggested formula based on the results of elemental analyses. Also, TGA denoted the formation of metal oxide as the end product from which the metal content is determined and found to be in satisfactory agreement with that obtained from analytical determination. The stages of decomposition, temperature ranges, calculated, and found mass losses as well as final products observed in each step of TGA/DTA curves are shown in table S2 "Supplementary material." The results show that all complexes decomposed in three steps (except $\mathbf{T_4}$ which decomposes in two steps). In the first step, the complexes showed mass loss within the temperature range 80–250°C corresponding to elimination of hydration, coordinated water and/or solvent molecules, associated with endothermic peaks within the range 49–105°C in the DTA thermogram. The second step from 130°C to 360°C with exothermic peak at 152–323°C is attributed to removal of anions attached to the metal. The final decomposition step from 195°C to 680°C with broad exothermic peak at 369–536°C included the thermal decomposition of the complexes [55] and loss of their organic parts with formation of the metal oxide as a final product.

### 3.6. *Cytotoxicity* in vitro *diagnostic*

Novel cancer agents or treatments are urgently needed to improve the outcome for the large number of patients who relapse after receiving the currently available cancer therapies [56]. In the present study, the effects of $\mathbf{T_1}$, $\mathbf{T_6}$, and $\mathbf{T_8}$ were examined on viability and proliferation of different human cancer cell lines. $\mathbf{T_8}$ was screened *in vitro* against five human cancer cell lines; HELA (cervical carcinoma cell line), HCT116 (colon carcinoma cell line), MCF7 (breast carcinoma cell line), HEP2 (larynx carcinoma cell line), and HEPG2 (liver carcinoma cell line). Complexes $\mathbf{T_1}$ and $\mathbf{T_6}$ were screened *in vitro* against HEPG2. The inhibitions of cell growth by the complexes were determined by SRB assay [24]. The complexes inhibit the growth of HELA, HCT116, MCF7, HEP2, and HEPG2 cells in a dose dependent manner (figures 3 and 4).

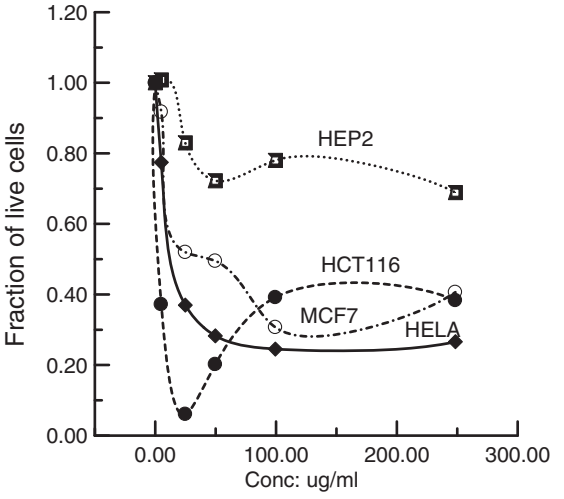


Figure 3. *In vitro* cytotoxicity of $\mathbf{T_8}$ against HELA, HCT116, MCF7, and HEP2 human cancer cell lines using different concentrations of the complex.

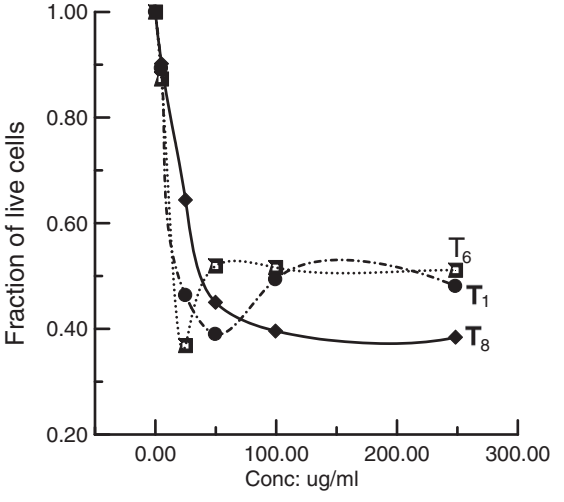


Figure 4. *In vitro* cytotoxicity of $\mathbf{T_1}$, $\mathbf{T_6}$, and $\mathbf{T_8}$ against HEPG2 human cancer cell line using different concentrations of the complexes.

Each data point is an average of three independent experiments and expressed as $M \pm SD$. Growth inhibition of 50% ($IC_{50}$) is calculated as the complex concentrations, which caused a 50% reduction in cell proliferation during the drug incubation [57]. The mean $IC_{50}$ is the concentration of drug that reduces cell growth by 50% under the experimental conditions and is the average with scanning electron microscopy from at least three independent determinations. $\mathbf{T_8}$ showed inhibition of cell viability giving $IC_{50}$ values of 18.2, 3.3, 41.4, and 44.1 $\mu g\,mL^{-1}$ against HELA, HCT116, MCF7, and HEPG2, respectively, but $\mathbf{T_8}$ did not reach $IC_{50}$ value for $HEP_2$. The cytotoxicity of $\mathbf{T_8}$ was found to be more effective toward HCT116 cell lines than that of doxorubicin

Table 3. Antimicrobial activities of $\mathbf{T_1}$, $\mathbf{T_2}$, and $\mathbf{T_7}$–$\mathbf{T_9}$.

| Compound | Inhibition zone diameter[a] (mm mg$^{-1}$ sample) | | | | |
|---|---|---|---|---|---|
| | *M. canis* (fungus) | *A. flavus* (fungus) | *C. albicans* (fungus) | *S. aureus* ($G^+$) | *E. coli* ($G^-$) |
| Tetracycline (antibacterial agent) | – | – | – | 31.13 ± 0.75 | 34.22 ± 0.64 |
| Amphotericin B (antifungal agent) | 19.23 ± 0.12 | 17.08 ± 0.11 | 19.06 ± 0.19 | – | – |
| Control: Ethyl alcohol | 0.0 ± 0.0 | 0.0 ± 0.0 | 0.0 ± 0.0 | 0.0 ± 0.0 | 0.0 ± 0.0 |
| $\mathbf{T_1}$ | N.D. | 13.06 ± 0.39 | 0.0 ± 0.0 | 14.00 ± 0.13 | 15.1 ± 0.21 |
| $\mathbf{T_2}$ | N.D. | N.D. | 20.69 ± 0.33 | N. D. | N.D. |
| $\mathbf{T_7}$ | 25.23 ± 0.16 | N.D. | 20.09 ± 0.72 | N.D | N.D. |
| $\mathbf{T_8}$ | N.D. | 13.16 ± 0.72 | 0.0 ± 0.0 | 15.19 ± 0.82 | 14.47 ± 0.34 |
| $\mathbf{T_9}$ | 39.43 ± 0.42 | N.D. | N.D. | N.D. | N.D. |

[a]Each experiment is conducted at least three times. Mean ± S.D. = standard deviation.



which gives $IC_{50}$ value of 3.7 μg mL$^{-1}$. These results indicate that $\mathbf{T_8}$ is more cytotoxic against HCT116 cancer cells compared to doxorubicin. $\mathbf{T_1}$ and $\mathbf{T_6}$ showed inhibition of cell viability giving $IC_{50}$ values of 24.3 and 17.5 μg mL$^{-1}$, respectively, against HEPG2 human cancer cell line (figures 3 and 4). The slight increase in the fraction of live cells at higher concentrations of the complexes in some cases may be attributed to increase of the cells viability due to association of the complexes at higher concentrations which decrease the activity of the metal complexes against the tumor cells [57]. As these results are preliminary, further study on the anti-tumor effects of these compounds is recommended.

### 3.7. In vitro *antimicrobial assay*

$\mathbf{T_1}$ and $\mathbf{T_8}$ were tested by a modified Kirby–Bauer diffusion method [24] and the results are presented in table 3. The activities of these compounds against *E. coli* and *S. aureus* were studied using tetracycline as a reference drug. The bactericidal activity of $\mathbf{T_1}$ and $\mathbf{T_8}$ are fairly good but low in comparison to the reference drug. The magnitude of antimicrobial properties of the complexes is related to the ease with which they participate in ligand exchange reactions [58]. For example, it has been speculated that weak M–O [59] and M–N [60] bonds might play an important role in exhibiting wider spectrum antimicrobial and antifungal activities and that the potential target sites for inhibition of bacterial and yeast growth by metal complexes might be sulfur containing residues of proteins [61].

Generally, the key factors determining antibacterial and antifungal activities of the complexes are the group coordinated to the metal atom (M–N, M–O, or M–S) and its bonding properties (i.e., the ease of ligand replacement), rather than the solid-state structure, solubility, charge, and degree of polymerization [62, 63].

Mueller–Hinton agar method was employed to test antifungal activities of $\mathbf{T_1}$, $\mathbf{T_2}$, and $\mathbf{T_7}$–$\mathbf{T_9}$ against three types of fungi, *C. albicans*, *A. flavus*, and *M. canis*, using Amphotericin B as a reference drug (table 3). The antifungal activities of $\mathbf{T_1}$ and $\mathbf{T_8}$ show inhibition ability against *A. flavus* only.

**$T_2$**, **$T_7$**, and **$T_9$** are more effective against *C. albicans*, *A. flavus*, and *M. canis* than Amphotericin B. The antimicrobial activity of the metal complexes is due to either killing the microbes or inhibiting their multiplication by blocking their active site [64].

## 4. Conclusion

Nine new complexes (**$T_1$**–**$T_9$**) were prepared by condensation of diacetylmonoxime with 2-amino-5-mercapto-1,3,4-thiadiazole, 2-amino-1,3,4-thiadiazole or 3-amino-5-methylisoxazole in the presence of Co(II) and Cu(II). The complexes were characterized by elemental and thermal analyses, molar conductance, spectral, and magnetic data. Sulfur, oxygen, and nitrogen participate in chelation with the metals. The investigated structures of the investigated complexes were supported by 3-D molecular modeling of **$T_1$** and **$T_6$**–**$T_9$**. Some of the Co(II) and Cu(II) complexes have better *in vitro* biological activities than the reference drugs when screened for antibacterial, antifungal, and cytotoxicity against human carcinoma cell line studies, thus giving a new thrust of these compounds in the field of metallo-drugs (bio-inorganic chemistry).



## References

[1] M.S. Gujral, P.M. Patnaik, R. Kaul, H.K. Parikh, C. Conradt, C.P. Tamhankar, G.V. Daftary. *Cancer Chemother. Pharmacol.*, **47**, 523 (2001).
[2] A. Mastrolorenzo, A. Scozzafava, C.T. Supuran. *Eur. J. Pharm. Sci.*, **11**, 325 (2000).
[3] A. Senff-Ribeiro, A. Echevarria, E.F. Silva, S.S. Veiga, M.B. Oliveira. *Anti-Cancer Drug*, **15**, 269 (2004).
[4] L. Ying, F. Haitao, Z. Yifan, W. Wuji. *J. Mater. Sci.*, **38**, 407 (2003).
[5] A. El-Shekeil, A. Al-Karbooly, F. Al-Yusufy. *J. Inorg. Organomet. Polym.*, **11**, 105 (2001).
[6] Y. Prashanthi, K. Kiranmai, N.J.P. Subhashini, Shivaraj. *Spectrochim. Acta A*, **70**, 30 (2008).
[7] R.C. Maurya, P. Patel, S. Rajput. *Synth. React. Inorg. Met.-Org. Chem.*, **33**, 817 (2003).
[8] R. Pogni, M.C. Baratto, A. Diaz, R. Basasi. *J. Inorg. Biochem.*, **79**, 333 (2000).
[9] M.B. Ferrari, F. Bisceglie, G. Pelosi, M. Sassi, P. Tarasconi, M. Cornia, S. Capacchi, R. Albertini, S. Pinelli. *J. Inorg. Biochem.*, **90**, 113 (2002).
[10] R.C. Mehrotra. In *Comprehensive Coordination Chemistry*, G. Wilkinson, R.D. Gillard, J.A. McCleverty (Eds), p. 269, Pergamon Press, Oxford (1987).
[11] A.G. Smith, P.A. Tasker, D.J. White. *Coord. Chem. Rev.*, **241**, 61 (2003).
[12] A.J.L. Pombeiro, Y.V. Kukushkin. In *Comprehensive Coordination Chemistry II*, J.A. McCleverty, T.C. Meyer (Eds), p. 2163, Elsevier, Amsterdam (2004).
[13] S. Sevagapandian, G. Rajagopal, K. Nehru, P. Athappan. *Trans. Met. Chem.*, **25**, 388 (2000).
[14] A. Balsamo, B. Macchia, A. Martinelli, E. Orlandini, A. Rossello, F. Macchia, G. Bocelli, P. Domiano. *Eur. J. Med. Chem.*, **25**, 227 (1990).
[15] M.V. Barybin, P.L. Diaconescu, C.C. Cummins. *Inorg. Chem.*, **40**, 2892 (2001).
[16] R.M. Srivastava, I.M. Brinn, J.O. Machura-Herrera, H.B. Faria, G.B. Carpenter, D. Andrade, C.G. Venkatesh, L.P.F. Morais. *J. Mol. Struct.*, **406**, 159 (1997).
[17] A. Chakravorty. *Coord. Chem. Rev.*, **13**, 1 (1974).
[18] M. Mohan, M. Kumar. *Polyhedron*, **4**, 1929 (1985).
[19] CS Chem 3-D Ultra Molecular Modeling and Analysis, Cambridge. Available online at: www.cambridgesoft.com (accessed March 23, 2011).
[20] R.C. Maurya, S. Rajput. *J. Mol. Struct.*, **794**, 24 (2006).
[21] A.M. Khedr, N.A. El-Wakiel, S. Jadon, V. Kumar. *J. Coord. Chem.*, **64**, 851 (2011).
[22] A.M. Khedr, S. Jadon, V. Kumar. *J. Coord. Chem.*, **64**, 1351 (2011).
[23] B.K. Singh, H.K. Rajour, A. Prakash, N. Bhojak. *Global J. Inorg. Chem.*, **1**, 65 (2010).
[24] P. Skehan, R. Storeng, D. Scudiero, A. Monks, J. McMahon, D. Vistica, J.T. Warren, H. Bokesch, S. Kenney, M.R. Boyd. *J. Natl. Cancer Inst.*, **82**, 1107 (1990).

[25] A.W. Bauer, W.M. Kirby, C. Sherris, M. Turck. *Am. J. Clin. Path.*, **45**, 493 (1966).
[26] M.A. Pfaller, L. Burmeister, M.A. Bartlett, M.G. Rinaldi. *J. Clin. Microbiol.*, **26**, 1437 (1988).
[27] National Committee for Clinical Laboratory Standards. *Performance Antimicrobial Susceptibility of Flavobacteria*, Vol. 41, NCCLS, Wayne, PA, USA (1997).
[28] National Committee for Clinical Laboratory Standards. *Reference Method for Broth Dilution Antifungal Susceptibility Testing of Conidium-forming Filamentous Fungi: Proposed Standard M38-A*, NCCLS, Wayne, PA, USA (2002).
[29] National Committee for Clinical Laboratory Standards. *Method for Antifungal Disk Diffusion Susceptibility Testing of Yeast: Proposed Guideline M44-P*, NCCLS, Wayne, PA, USA (2003).
[30] National Committee for Clinical Laboratory Standards. *Methods for Dilution Antimicrobial Susceptibility Tests for Bacteria that Grow Aerobically. Approved Standard M7-A3*, NCCLS, Villanova, PA (1993).
[31] L.D. Liebowitz, H.R. Ashbee, E.G.V. Evans, Y. Chong, N. Mallatova, M. Zaidi, D. Gibbs. *Diagn. Microbiol. Infect. Dis.*, **4**, 27 (2001).
[32] M.J. Matar, L. Ostrosky-Zeichner, V.L. Paetznick, J.R. Rodriguez, E. Chen, J.H. Rex. *Antimicrob. Agents Chemother.*, **47**, 1647 (2003).
[33] A.I. Vogel. *A Text Book of Quantitative Inorganic Analysis*, Longmans, London (1969).
[34] S.F.A. Kettle. *Coordination Compounds*, Thomas Nelson & Sons, Nashville, TN (1969).
[35] P.K. Rai, R.N. Prasad. *Monatsh. Chem.*, **125**, 385 (1994).
[36] E. Gao, S. Bi, H. Sun, H. Liv. *Synth. React. Inorg. Met.-Org. Chem.*, **27**, 115 (1997).
[37] K. Nakamoto. *Infrared Spectra of Inorganic and Coordination Compounds*, Wiley-Interscience, New York (1970).
[38] A.C. Fabretti, G.C. Franchini, G. Peyronel. *Trans. Met. Chem.*, **7**, 306 (1982).
[39] M. Moszner, M. Kubiak, J.J. Ziółkowski. *Inorg. Chim. Acta*, **357**, 155 (2004).
[40] M. Kayaa, C. Yenikayaa, A.T. Colaka, F. Colakb. *Russ. J. Chem.*, **78**, 9 (2008).
[41] J. Sanmartin, M.R. Bermejo, A.M. Garia-Deibe, M. Maneiro, C. Lage, A.J. Costa-Filho. *Polyhedron*, **19**, 185 (2000).
[42] K.S. Abu-Melha, N.M. El-Metwally. *Trans. Met. Chem.*, **32**, 828 (2007).
[43] Z.H. Abd El-Wahab, M.R. El-Sarrag. *Spectrochim. Acta A*, **60**, 271 (2004).
[44] K.K. Narang, V.P. Singh. *Trans. Met. Chem.*, **21**, 507 (1997).
[45] S.M. Abu-El-Wafa, N.A. El-Wakiel, R.M. Issa, R.A. Mansour. *J. Coord. Chem.*, **58**, 683 (2005).
[46] K.Y. El-Baradie. *Monatsh. Chem.*, **136**, 1139 (2005).
[47] B.K. Singh, P. Mishra, B.S. Garg. *Main Group Chem.*, **5**, 163 (2006).
[48] S.S. Kandil. *Trans. Met. Chem.*, **23**, 461 (1998).
[49] A.B.P. Lever. *Inorganic Electronic Spectroscopy*, 2nd Edn, Elsevier, Amsterdam (1984).
[50] E.W. Ainscough, A.M. Brodie, A.J. Dobbs, J.D. Ranford, J.M. Waters. *Inorg. Chim. Acta*, **267**, 27 (1998).
[51] F.K. Kneubuhl. *J. Chem. Phys.*, **33**, 1074 (1960).
[52] V. Ravindar, S.J. Swamy, S.S. Srihari, P. Longaiah. *Polyhedron*, **4**, 1511 (1985).
[53] P. Guerriero, S. Tamburini, P.A. Vigato. *Coord. Chem. Rev.*, **139**, 17 (1995).
[54] M. Badea, A. Emandi, D. Marinescu, E. Cristurean, R. Olar, A. Braileanu, P. Budrugeac, E. Segal. *J. Therm. Anal. Calorim.*, **72**, 525 (2003).
[55] K.Y. El-Baradie, M. Gaber. *Chem. Pap.*, **57**, 317 (2003).
[56] A.S. Sultan, H. Brim, Z.A. Sherif. *Cancer Sci.*, **2**, 272 (2008).
[57] S.H. Etaiw, S.A. Amer, M.M. El-Bendary. *J. Inorg. Organomet. Polym.*, **21**, 110 (2011).
[58] I. Tsyba, B.B. Mui, R. Bau, R. Noguchi, K. Nomiya. *Inorg. Chem.*, **42**, 8028 (2003).
[59] K. Nomiya, H. Yokoyama. *J. Chem. Soc., Dalton Trans.*, 2483 (2002).
[60] K. Nomiya, S. Takahashi, R. Noguchi, S. Nemoto, T. Takayama, M. Oda. *Inorg. Chem.*, **39**, 3301 (2000).
[61] K. Nomiya, H. Yokoyama. *J. Chem. Soc., Dalton Trans.*, 2091 (2000).
[62] K. Nomiya, K. Tsuda, T. Sudoh, M. Oda. *J. Inorg. Biochem.*, **68**, 39 (1997).
[63] K. Nomiya, K. Tsuda, N.C. Kasuga. *J. Chem. Soc., Dalton Trans.*, 1653 (1998).
[64] W. Rehman, M.K. Baloch, A. Badshah. *Eur. J. Med. Chem.*, **43**, 2380 (2008).